Manuscript 5315 – Revision 1

The speciation of carbon monoxide in silicate melts and glasses

TAKAHIRO YOSHIOKA, CATHERINE McCAMMON, SVYATOSLAV SHCHEKA, AND HANS KEPPLER*

Bayerisches Geoinstitut, Universität Bayreuth, 95440 Bayreuth, Germany
* E-mail: Hans.Keppler@uni-bayreuth.de

ABSTRACT

We have studied the speciation of carbon monoxide in both Fe-bearing and Fe-free basaltic glasses using Raman, FTIR, and Mössbauer spectroscopy. We show that a band at 2110 cm^{-1} in the Raman spectrum and another band at 2210 cm^{-1} in the FTIR spectrum occur both in the Fe-bearing and Fe-free samples, implying that they cannot be due to any Fe-bearing species. This observation is consistent with ^{57}Fe Mössbauer spectra, which do not show any evidence for Fe species with zero isomer shift, as expected for carbonyls. Thermodynamic calculations show that iron carbonyl in basaltic melts under crustal and upper mantle conditions may only be a trace species. Rather than being due to distinct chemical species, the range of vibrational frequencies observed for carbon monoxide in silicate glasses appears to be due to rather subtle interactions of the CO molecule with the matrix. Similar effects are known from the extensive literature on carbon monoxide adsorption on oxides and other surfaces. In the melt at high temperature, there is likely little interaction of the CO molecule with the silicate matrix and solubility may be largely controlled by pressure, temperature, and the overall polymerization or ionic porosity of the melt.

Keywords. Silicate melt, carbon monoxide, iron, carbonyl, Raman, Mössbauer

INTRODUCTION

Carbon dioxide is an important component of volcanic gases, usually second in abundance only to water. Due to its low solubility in silicate melts at low pressure, CO_2 may drive bubble nucleation during eruptions and the melting point depression induced by CO_2 plays an important role in stabilizing low-degree partial melts in the mantle (e.g. Wyllie and Huang 1976). Accordingly, carbon dioxide solubility in silicate melts has been extensively studied (Ni and Keppler 2013 and references therein). In contrast to CO_2, the solubility of carbon monoxide (CO) in silicate melts has received relatively little attention, probably because it is only a trace component in volcanic gases (Symonds et al. 1994) and because thermodynamic calculations suggest that under the oxygen fugacities prevailing in the Earth today, its abundance in crustal and upper mantle fluids is low (e.g. Frost and McCammon 2008). However, carbon monoxide could be an important species of carbon during planetary degasing under reducing conditions, e.g. on the Moon, during core formation on Earth, or perhaps even today in the reduced, deep mantle (e.g. Wetzel et al. 2013; Hirschmann 2013).

Pawley et al. (1992) suggested that carbon monoxide is much less soluble than carbon dioxide in a basaltic melt at 1200 °C and 500 to 1500 bar. A similar conclusion was reached by Morizet et al. (2010). Brooker et al. (1999) detected dissolved CO in reduced glasses prepared along the $NaAlO_2$-SiO_2 join by FTIR and NMR spectroscopy. In the NMR spectrum, a peak at a chemical shift of 185 ppm was assigned to CO; FTIR spectra showed a band between about 2160 and 2180 cm^{-1}, depending on the composition of the glass matrix. Notably, this absorption frequency is significantly higher than for CO in the gas phase (2143 cm^{-1}). Wetzel et al. (2013) reported a band at 2110 cm^{-1} in the Raman spectra of reduced, carbon-bearing basalt glasses and attributed it to iron pentacarbonyl $Fe(CO)_5$. They inferred that $Fe(CO)_5$ is the main species of reduced carbon in these glasses. Stanley et al. (2014) suggested that a band at 2205 cm^{-1} in the infrared spectrum in a graphite-saturated basalt could also be due to a carbonyl species.

The stability of carbonyl species in silicate melts and glasses could have important implications for the behavior of carbon, since carbon solubility would then be strongly coupled to the availability of iron. Carbonyls are molecules containing carbon monoxide coordinated to a transition metal. Typical examples are $Ni(CO)_4$ and $Fe(CO)_5$. Stable carbonyls are only known from the central block of the transition metals in the periodic table, where iron is the only element sufficiently abundant to be relevant for discussing the potential stability of carbonyls in natural silicate melts. The metal atom in simple carbonyls has the formal oxidation state of zero, which is

related to an unusual mechanism of chemical bonding (e.g. Greenwood and Earnshaw 1984). An electron pair from the carbon atom is donated to the metal atom to form a σ bond; this bond is strengthened by a back-donation of d electrons from the metal atom into the anti-bonding orbitals of the CO molecule. Populating the anti-bonding orbitals of CO weakens the bond between carbon and oxygen and therefore usually causes the vibrational frequency of CO in a carbonyl to be shifted downwards relative to the free CO molecule.

In this study, we combined Raman, FTIR, and Mössbauer spectroscopy on Fe-bearing and Fe-free basaltic glasses containing reduced carbon in order to investigate the dissolution mechanism of carbon monoxide in silicate melts and glasses.

EXPERIMENTAL AND ANALYTICAL METHODS

Two different synthetic glasses were used as starting materials. One was equivalent in composition to the lunar green glass used by Wetzel et al. (2013). A second glass had the same composition, with the exception that all FeO (total iron expressed as FeO) was replaced by an equimolar mixture of CaO and MgO. The glasses were prepared from stoichiometric mixtures of high-purity oxides and carbonates. The mixtures were homogenized and first decarbonated by slowly heating them over 12 hours to 1100 °C. They were then re-melted for 1 hour at 1600 °C and quenched in distilled water. Microprobe analyses of the clear, crystal-free glasses are given in the footnote of Table 1. Before the actual high-pressure experiments, the Fe-bearing glass was first wrapped in an iron foil and reduced in a CO-CO_2 gas mixture at 1300 °C for 3 hours and an oxygen fugacity of one log unit below the iron-wustite buffer. This is the same oxygen fugacity as expected to prevail in the following piston cylinder experiments in equilibrium with Fe metal and graphite (Wetzel et al. 2013).

High-pressure experiments (Table 1) were carried out in an end-loaded piston-cylinder apparatus at 10 kbar and 1450 – 1530 °C for 2 hours. Glass powder was loaded into graphite capsules inside platinum rhodium ($Pt_{95}Rh_5$) capsules with 5 mm diameter, 10 mm length and 0.3 mm wall thickness. Only in experiments with the Fe-bearing glass, some wire of metallic iron was also added to the charge to buffer oxygen fugacity. No water was added in any of the experiments. Some experiments were also carried out with a trace (0.5 wt.%) of $^{57}Fe_2O_3$ added to the Fe-free glass. No iron metal was added in these runs. All experiments were quenched to room temperature within a few seconds by turning off the power to the heater. Run products were

106 usually clear glasses, only in a few runs minor quench crystallization of olivine was observed. No
107 gas bubbles were observed in the glasses and we therefore assume that all volatiles dissolved
108 under run conditions are fully conserved in the glass.
109
110 FTIR spectra were measured with a Bruker IRscopeI attached to a Bruker IFS120HR
111 spectrometer. The optics of the spectrometer were kept under vacuum during the measurement,
112 while the microscope was permanently purged with purified air. Measurements were carried out
113 on doubly polished platelets of run product glasses of 248 to 254 μm thickness. For each
114 measurement, 200 scans were accumulated with 4 cm^{-1} resolution, using a tungsten light source, a
115 CaF_2 beam splitter and a narrow-band MCT-detector. The spot size was limited to 120 μm by an
116 aperture in the rear focal plane of the 15 X Cassegranian objective.
117
118 Raman spectra were measured on the same samples as used for FTIR spectroscopy using a
119 confocal Horiba Jobin-Yvon Labram 800HR UV spectrometer with the 514 nm line of an Ar
120 laser at 200 mW output power as excitation source. Spectra were measured with a 50X objective,
121 a 1800 mm^{-1} grating, and a Peltier-cooled CCD detector, with an optical resolution of 2 cm^{-1} and
122 an accumulation time of 20 times 10 seconds. A reference spectrum of pure $Fe(CO)_5$ (supplied by
123 Sigma-Aldrich) inside a glass cuvette was also measured with the same system, but with an
124 accumulation time of only 2 times 5 seconds and < 10 mW laser power, to avoid evaporating or
125 decomposing the liquid.
126
127 Mössbauer spectra were measured at room temperature in transmission mode on a constant
128 acceleration Mössbauer spectrometer with a nominal 370 MBq ^{57}Co high specific activity source
129 in a 12 μm thick Rh matrix. The velocity scale was calibrated relative to Fe foil. The
130 dimensionless thickness of the Fe-bearing and the $^{57}Fe_2O_3$-doped sample was 2.9 and 4.9,
131 respectively. Spectra were collected for about 1 day. Spectra were fitted using the xVBF method
132 (e.g., Lagarec and Rancourt 1997) as implemented by MossA software (Prescher et al. 2012).
133
134 **RESULTS AND DISCUSSION**
135
136 **Raman and infrared spectra**
137 Raman and infrared spectra of both Fe-bearing and Fe-free glasses are shown in Figure 1. The
138 Raman spectra (Fig. 1 a) of the Fe-bearing glasses show a peak at 2110 cm^{-1}, very similar to the
139 peak assigned by Wetzel et al. (2013) to $Fe(CO)_5$. Additional peaks at 1350 cm^{-1} and 1590 cm^{-1}
140 are due to traces of graphite, the band near 3600 cm^{-1} is due to dissolved OH. Methane (CH_4, near

2917 cm^{-1}) is not detectable. However, essentially the same bands, including the one at 2110 cm^{-1} are also seen in the Raman spectrum of the Fe-free glass. This observation rules out any assignment of this band to a Fe-bearing species. Moreover, while a band near this frequency does indeed occur in the reference spectrum of pure $Fe(CO)_5$ shown in Figure 1 b, a strong $Fe(CO)_5$ band near 2014 cm^{-1} (e.g. Bigorgne 1970; Jones et al. 1972) is not seen in the spectra of the CO-bearing glasses.

The infrared spectra (Fig. 1 c) of the Fe-bearing glasses show a peak near 2210 cm^{-1}, that is very similar to a band at 2205 cm^{-1} observed by Stanley et al. (2014), which was tentatively assigned by them to a Fe carbonyl anion. In addition, a band due to dissolved OH occurs near 3500 cm^{-1}, corresponding to a water content of about 0.15 wt. %, using the extinction coefficient of Dixon et al. (1988). No clear evidence for carbonate is seen in the infrared spectra. Unlike in the study of Wetzel et al. (2013), no band can be detected near 2110 cm^{-1}; however, this band is also very weak in the spectra reported by those authors. The 2210 cm^{-1} band also occurs in the spectrum of the Fe-free glass, again ruling out any assignment to a Fe-bearing species.

Mössbauer spectra

Mössbauer spectroscopy should readily allow the identification of any Fe-carbonyl species in a glass, because the formal oxidation state of Fe in carbonyls is zero. This causes the isomer shift of Fe-carbonyl species to be nearly zero (Kalvius et al. 1962; Herber et al. 1963), which is easily distinguishable from the normal isomer shift of Fe^{2+} or Fe^{3+} in glasses (e.g. Virgo and Mysen 1985). Figure 2a shows the Mössbauer spectrum of a graphite-saturated, Fe-bearing glass. Only the normal doublet of Fe^{2+} is seen, with an isomer shift of 1.04 mm/s and a quadrupolar splitting of 1.96 mm/s. However, from these data, one cannot conclude that iron carbonyl species are absent from the sample, since the Fe concentration (8.69 wt.% bulk FeO) is much higher than the concentration of dissolved CO. The latter cannot be directly inferred from spectroscopic data, as the infrared extinction coefficient of CO in glass is not known; however, it is likely that CO concentration is in the order of hundreds to a few thousand ppm for the conditions where the samples were synthesized (e.g. Wetzel et al. 2013; Stanley et al. 2014). Therefore, a glass was prepared with a much lower bulk iron content (0.5 wt. % FeO), where all iron was added as $^{57}Fe_2O_3$. The Raman and infrared spectra of this glass showed the same bands at 2110 and 2210 cm^{-1} as the glass with higher Fe content. The Mössbauer spectrum (Fig. 2 b) is also virtually indistinguishable from the spectrum of the Fe-rich glass. If iron carbonyls were major CO species in this sample, they should represent a considerable fraction of the total iron, and therefore an enhancement of absorption near zero isomer shift should be seen. This is not observed.

176

177 **Thermodynamic considerations**

178 The thermodynamic properties of iron pentacarbonyl are known from a combination of
179 calorimetric and spectroscopic data (Behrens 1977). By combining them with standard state
180 thermodynamic data for carbon monoxide and iron metal (Robie and Hemingway 1995), the
181 equilibrium constant K for the reaction

182

183 $$Fe + 5\ CO = Fe(CO)_5$$

184

185 can readily be calculated. This yields $\ln K = -66.71 + 20363/T$, where T is temperature in Kelvin.
186 The equilibrium constant is defined as

187

188 $$K = \frac{f_{Fe(CO)_5}}{a_{Fe} f_{CO}^5}$$

189

190 where f are fugacities and a_{Fe} is the activity of iron. Assuming equilibrium with metallic iron – as
191 in some of our experiments – a_{Fe} becomes 1 and the fugacity of the pentacarbonyl can easily be
192 calculated for a given CO fugacity. The results of these calculations are shown in Figure 3. For
193 all plausible conditions of temperature and CO fugacity in the crust and upper mantle, the ratio of
194 the pentacarbonyl fugacity to the CO fugacity is very low, implying that $Fe(CO)_5$ may only be a
195 trace species in a gas phase at run conditions. The ratio of $Fe(CO)_5$ to CO in a coexisting silicate
196 melt could potentially be higher, due to preferential partitioning of $Fe(CO)_5$ into the melt.
197 However, the fugacity ratios in the gas phase are so unfavorable for the formation of $Fe(CO)_5$ that
198 this effect is unlikely to stabilize significant amount of iron carbonyl in the melt. The high
199 volatility of $Fe(CO)_5$ (boiling point of 103 °C at 1 bar) also makes preferential partitioning into a
200 silicate melt in equilibrium with a gas phase unlikely. For conditions where the melt is not in
201 equilibrium with metallic iron, $Fe(CO)_5$ abundances will be even lower. For more complicated
202 (polynuclear) Fe carbonyl species, thermodynamic data are lacking; however, the main reason for
203 the low stability of $Fe(CO)_5$ at high temperatures is the strongly negative entropy of formation
204 from Fe and CO ($\Delta S^\circ = -574.3$ J/mol K for $Fe(CO)_5$ gas). For larger, more complicated Fe
205 carbonyl species, this number will be even more negative, making their stability at high
206 temperatures very unlikely.

207

208

209

A comparison with carbon monoxide adsorbed on surfaces

The bands in the 2100 cm^{-1} to 2200 cm^{-1} range observed here and in previous studies (Brooker et al. 1999; Wetzel et al. 2013; Stanley et al. 2014) are very likely due to some kind of CO dissolved in the glass, as they occur in a frequency range where normally only triple-bonded light elements are observed. Vibrational frequencies of acetylene HCCH, hydrogen cyanide HCN, and derived species may occur in a similar range. However, the C-H bands of acetylene are not observed and our samples do not contain measurable nitrogen, so assigning these bands to carbon monoxide is the only plausible possibility. This would imply that the vibrational frequencies of CO in glasses are much more strongly affected by the glass matrix than those of CO_2. For molecular carbon dioxide in glasses, the infrared spectra always show a band very close to the antisymmetric stretching frequency of the free CO_2 molecule (2349 cm^{-1}; Ni and Keppler 2013). The stronger interaction of CO with the silicate matrix may be related to the fact that CO has a permanent dipole moment, which CO_2 does not have. Moreover, the CO has antibonding molecular orbitals at relatively low energy (e.g. Greenwood and Earnshaw 1984), so that it can accept electron density, which reduces the bond strength and therefore the stretching frequency.

Some insights into possible interactions between the CO molecule with the glass matrix may be gained from the extensive literature on CO adsorption on surfaces. While the chemical bonding of CO on a surface may not be exactly the same as the interaction of the CO molecule with a surrounding glass matrix, the data provide a useful guide for understanding the relationship between chemical bonding and vibrational frequencies. Raman frequency shifts for CO adsorbed on surfaces have been reported, which are even larger than the shifts observed in glasses. Interestingly, both shifts to higher and to lower frequencies are observed and they also occur in systems without transition metals and systems where carbonyls are not stable. Bordiga et al. (1995) observed that the stretching frequency of CO adsorbed on a zeolite (mordenite) shifts from 2155 cm^{-1} to 2188 cm^{-1}, depending on the alkali ion present. Similar shifts were observed for the adsorption on a titanosilicate (Zecchina et al. 1999). Several theoretical studies have investigated the adsorption of CO on the surface of MgO crystals (Neymann and Rösch 1992, 1993; Pacchioni et al. 1992). Interestingly, these models predict an increase of the CO stretching frequency, if the carbon atom docks to the surface, while a decrease in frequency is predicted, if CO is coordinated to the surface by the oxygen atom. Predicted frequency shifts range from – 124 cm^{-1} to + 99 cm^{-1} relative to the stretching frequency of the free CO molecule. The effect is mainly attributed to electrostatic fields acting on the CO dipole, rather than to direct chemical bonding to the surface. Adsorption experiments on silver surfaces also show some interesting effects. Note that no stable silver carbonyls are known and silver, being a noble metal, is not

expected to easily form chemical bonds. Yamamoto and Nanba (1988) observed that they could reduce the stretching frequency of CO adsorbed on a silver film by 29 or 23 cm^{-1}, respectively, by co-adsorbing xenon and krypton. Mahoney et al. (1984) reported that they could induce large shifts in the stretching frequency of CO adsorbed on a silver electrode simply by changing the chemical potential on the electrode. This effect, sometimes called "Stark tuning" has also been observed for other electrode materials (Zhou and Weaver 1996). All of these observations suggest that the CO stretching frequency is extremely sensitive to very subtle changes in the environment of the molecule.

IMPLICATIONS

The experimental data presented here imply that bands observed in the 2100 – 2200 cm^{-1} range of the Raman and infrared spectra of reduced, carbon-bearing glasses are not due to several, distinct chemical species, but caused by CO molecules weakly interacting with the matrix. This conclusion is consistent with the extensive literature on CO adsorbed on surfaces. In silicate melt at high temperature, these weak interactions are small compared to thermal energy and therefore, the CO molecule probably dissolves in the melt with little interaction with the matrix. CO solubility is therefore likely a simple function of pressure, temperature and the bulk structure of the silicate melt, as expressed by the degree of polymerization or ionic porosity. However, theoretical studies of surface adsorbed CO suggest that CO molecules with different stretching frequencies may have very different infrared absorption coefficients (Neyman and Rösch, 1992), which may require matrix-specific calibrations for measuring CO in silicate glasses by infrared spectroscopy.

ACKNOWLEDGEMENTS

Constructive reviews by Jim Webster, Alexander Borisov, Fabrice Gaillard, and Ian Swainson helped to improve the manuscript.

REFERENCES CITED

Behrens, R.G. (1977) Thermodynamics of transition metal carbonyls I. $Fe(CO)_5$, $Ru(CO)_5$, $Os(CO)_5$. Journal of the Less-common Metals, 56, 55-68.

Bigorgne, M. (1970) Étude spectroscopique Raman et infrarouge de $Fe(CO)_5$, $Fe(CO)_4L$ et trans-$Fe(CO)_3L_2$ (L=PMe_3, $AsMe_3$, $SbMe_3$). I. Attribution des bandes de $Fe(CO)_5$. Journal of Organometallic Chemistry, 24, 211-229.

Bordiga, S., Lamberti, C., Geobaldo, F., and Zecchina, A. (1995) Fourier-transform infrared study of CO adsorbed at 77 K on H-Mordenite and alkali-metal exchanged mordenites. Langmuir, 11, 527-533

Brooker, R.A., Kohn, S.C., Holloway, J.R., McMillan, P.F., and Carroll, M.R. (1999) Solubility, speciation and dissolution mechanism for CO_2 in melts on the $NaAlO_2$-SiO_2 join. Geochimica et Cosmochimica Acta, 63, 3549-3565.

Dixon, J.E., Stolper, E.M., and Delaney, J.R. (1988) Infrared spectroscopic measurements of CO_2 and H_2O in Juan de Fuca Ridge basaltic glasses. Earth and Planetary Science Letters, 90, 87-104.

Frost, D.J., and McCammon, C.A. (2008) The redox state of Earth´s mantle. Annual Review of Earth and Planetary Sciences, 36, 389-420.

Greenwood, N.N., and Earnshaw, A. (1984) Chemistry of the Elements. Pergamon Press.

Herber, R.H., Kingston, W.R., and Wertheim, G.K. (1963) Mossbauer effect in iron pentacarbonyl and related carbonyls. Inorganic Chemistry, 2, 153-158.

Hirschmann, M.M. (2013) Fe-carbonyl is a key player in planetary magmas. Proceedings of the National Academy of Sciences of the United States of America, 110, 7967-7968.

Jones, L.H., McDowell, R.S., Goldblatt, M., and Swanson, B.I. (1972) Potential constants of iron pentacarbonyl from vibrational spectra of isotopic species. The Journal of Chemical Physics, 57, 2050-2064.

Kalvius, M., Zahn, U., Kienle, P., and Eichner, H. (1962) Hyperfeinstruktur des 14,5 keV-Zustandes von Fe^{57}, gebunden in verschiedenen Eisencarbonylen. Zeitschrift für Naturforschung, A 17, 494-499.

313 Lagarec, K., and Rancourt, D.G. (1997) Extended Voigt-based analytic lineshape method for
314 determining N-dimensional correlated hyperfine parameter distributions in Mössbauer
315 spectroscopy. Nuclear Instruments and Methods in Physics Research, B 129, 266-280
316
317 Mahoney, M.R., Howard, M.W., and Cooney, R.P. (1984) Raman spectra of carbon monoxide
318 adsorbed on silver electrodes. Journal of Electroanalytical Chemistry, 161, 163-167.
319
320 Morizet, Y., Paris, M., Gaillard, F., and Scaillet, B. (2010) C-O-H fluid solubility in haplobasalt
321 under reducing conditions: An experimental study. Chemical Geology, 279, 1-16.
322
323 Neyman, K.M., and Rösch, N. (1992) CO bonding and vibrational modes on a perfect MgO (001)
324 surface: LCGTO-LDF model cluster investigation. Chemical Physics, 168, 267-280.
325
326 Neyman, K.M., and Rösch, N. (1993) Bonding and vibration of CO molecules adsorbed on low-
327 coordinated sites on MgO: a LCGTO-LDF cluster investigation. Surface Science, 297, 223-234.
328
329 Ni, H., and Keppler, H. (2013) Carbon in silicate melts. Reviews in Mineralogy and
330 Geochemistry, 75, 251-287.
331
332 Pacchioni, G., and Cogliandro, G. (1992) Molecular orbital cluster model study of bonding and
333 vibrations of CO adsorbed on MgO surface. International Journal of Quantum Chemistry, 42,
334 1115-1139.
335
336 Pawley, A.R., Holloway, J.R., and McMillan, P.F. (1992) The effect of oxygen fugacity on the
337 solubility of carbon oxygen fluids in basaltic melt. Earth and Planetary Science Letters, 110, 213-
338 225.
339
340 Prescher, C., McCammon, C., and Dubrovinsky, L. (2012) MossA - a program for analyzing
341 energy-domain Mossbauer spectra from conventional and synchrotron sources. Journal of
342 Applied Crystallography, 45, 329-331
343
344 Robie, R.A., and Hemingway, B.S. (1995) Thermodynamic Properties of Minerals and Related
345 Substances at 298.15 K and 1 bar (10^5 Pascals) Pressure and at Higher Temperatures. United
346 States Geological Survey Bulletin 2131.
347

348 Stanley, B.D., Hirschmann, M.M., and Withers, A.C. (2014) Solubility of C-O-H volatiles in
349 graphite-saturated martian basalts. Geochimica et Cosmochimica Acta, 129, 54-76.
350
351 Symonds, R.B., Rose, W.I., Bluth, G.J.S., and Gerlach, T.M. (1994) Volcanic-gas studies:
352 Methods, results, and applications. Reviews in Mineralogy, 30, 1-66.
353
354 Virgo, D., and Mysen, B.O. (1985) The structural state of iron in oxidized vs. reduced glasses at
355 1 atm: A ^{57}Fe Mössbauer study. Physics and Chemistry of Minerals, 12, 65-76.
356
357 Wetzel, D.T., Rutherford, M.J., Jacobsen, S.D., Hauri, E.H., and Saal, A.E. (2013) Degasing of
358 reduced carbon from planetary basalts. Proceedings of the National Academy of Sciences of the
359 United States of America, 110, 8010-8013.
360
361 Wyllie, P.J., and Huang, W.L. (1976) Carbonation and melting reactions in system CaO-MgO-
362 SiO_2-CO_2 at mantle pressures with geophysical and petrological applications. Contributions to
363 Mineralogy and Petrology, 54, 79-107.
364
365 Yamamoto, I., and Nanba, T. (1988) Change in the stretching frequency of a CO molecule
366 absorbed on a silver film induced by coadsorption. Surface Science, 202, 377-387.
367
368 Zecchina, A., Otero Areán, C., Turnes Palomona, G., Geobaldo, F., Lamberti, C., Spoto, G., and
369 Bordiga, S. (1999) The vibrational spectroscopy of H_2, N_2, CO and NO adsorbed on the
370 titanosilicate molecular sieve ETS-10. Physical Chemistry Chemical Physics, 1, 1649-1657.
371
372 Zhou, S., and Weaver, M.J. (1996) Potential dependent metal-adsorbate stretching frequencies for
373 carbon monoxide on transition metal electrodes: Chemical bonding versus electrostatic field
374 effects. Journal of Physical Chemistry, 100, 4237-4242
375

376 **Table 1.** Synthesis conditions of glasses and a summary of the Raman and infrared bands observed in them.

377

Run no.	Starting material	P	T	Duration	Crystals[§]	FTIR (cm^{-1})		Raman spectroscopy (cm^{-1})							
		(GPa)	(°C)	(hours)		2025	2210	1350	1590	1725	2110	2710	2965	3075	3570
A717	Fe-bearing glass*	1	1530	2			✔	✔	✔		✔	✔			✔
B809	Fe-bearing glass*	1	1450	2			✔	✔	✔		✔				✔
A726	Fe-free glass**	1	1530	2				✔	✔		✔	✔			✔
A727	Fe-free glass**	1	1450	2	✔	✔	✔	✔	✔		✔	✔			✔
A732	Fe-free glass**	1	1530	2	✔		✔	✔	✔		✔	✔			✔
A751	^{57}Fe-doped glass[#]	1	1530	2			✔	✔	✔	✔	✔	✔	✔	✔	✔
A752	^{57}Fe-doped glass[#]	1	1530	2	✔		✔	✔	✔		✔	✔	✔		✔

* 44.65 wt% SiO_2, 8.69 wt% Al_2O_3, 23.12 wt% MgO, 8.71 wt% CaO, 14.57 wt% FeO, 0.32 wt% TiO_2,.

** 48.00 wt% SiO_2, 9.78 wt% Al_2O_3, 24.44 wt% MgO, 16.50 wt% CaO, 0.37 wt% TiO_2.

[#] Fe-free glass doped with 0.5 wt.% of $^{57}Fe_2O_3$

[§] Small amounts of quench crystals of olivine in some glasses

All runs were saturated with graphite (the capsule material); runs A717 and B809 were also in equilibrium with iron metal

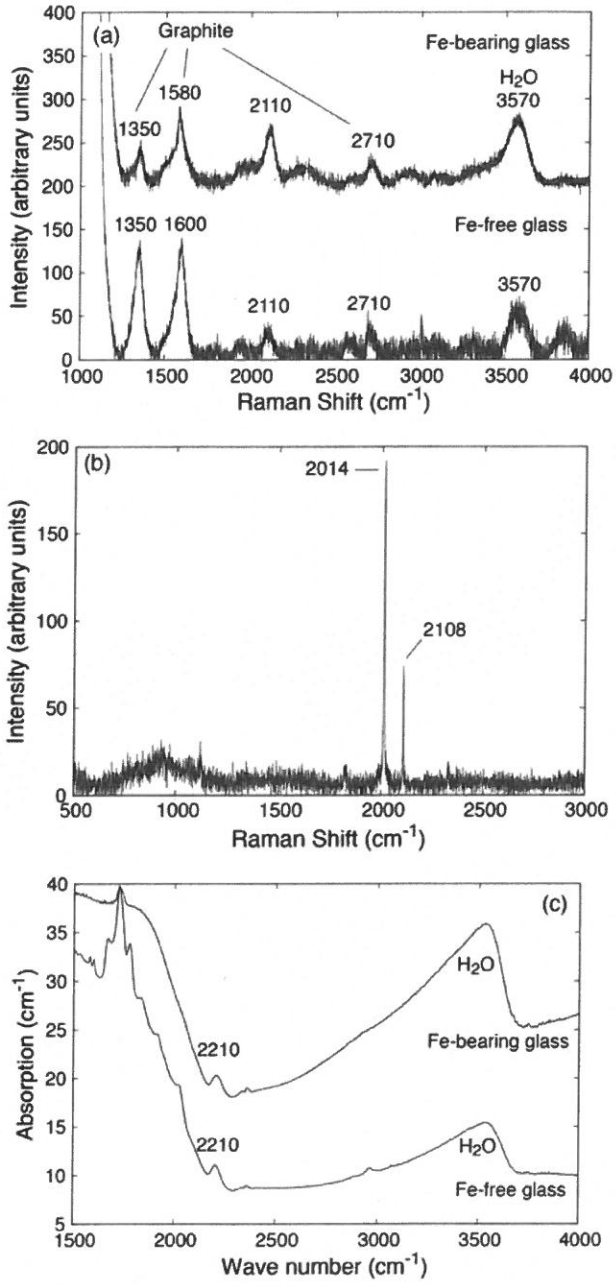

Fig. 1. Raman and infrared spectra of graphite-saturated glasses and of iron pentacarbonyl $Fe(CO)_5$. a) Raman spectra of a Fe-bearing and Fe-free, graphite saturated glass; b) Raman spectrum of pure $Fe(CO)_5$, supplied by Sigma-Aldrich; c) infrared spectra of a Fe-bearing and Fe-free, graphite saturated glass.

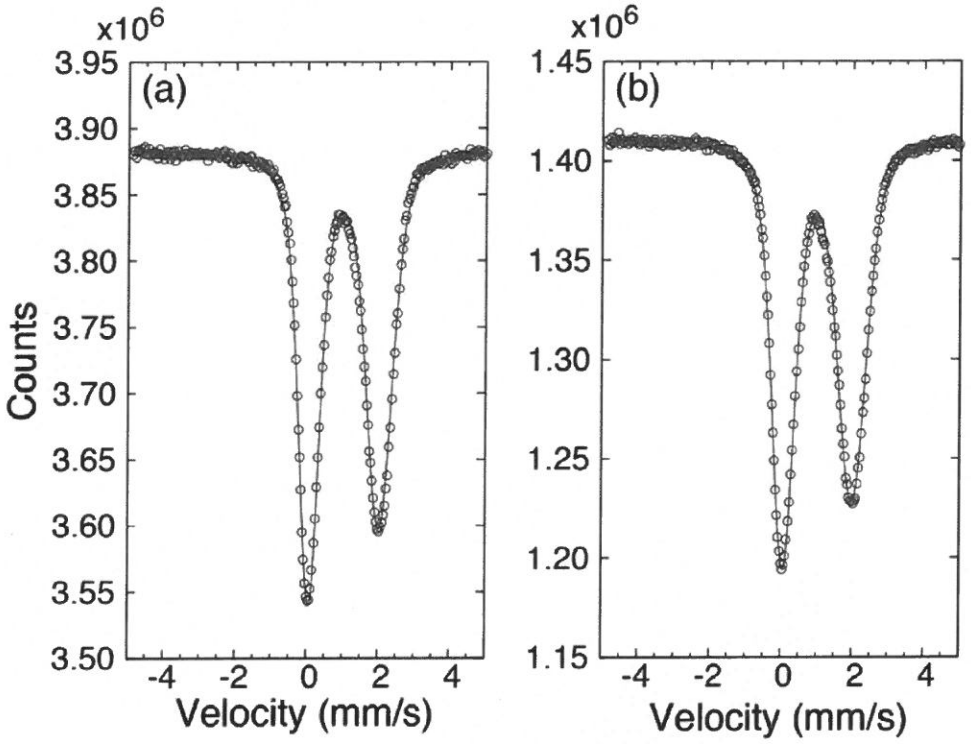

Fig. 2. ^{57}Fe Mössbauer spectra of two graphite-saturated glasses. a) Glass with 8.69 wt. % FeO, no isotopic enrichment, sample thickness 253 μm; b) glass with 0.5 wt. % ^{57}FeO, sample thickness 252 μm.

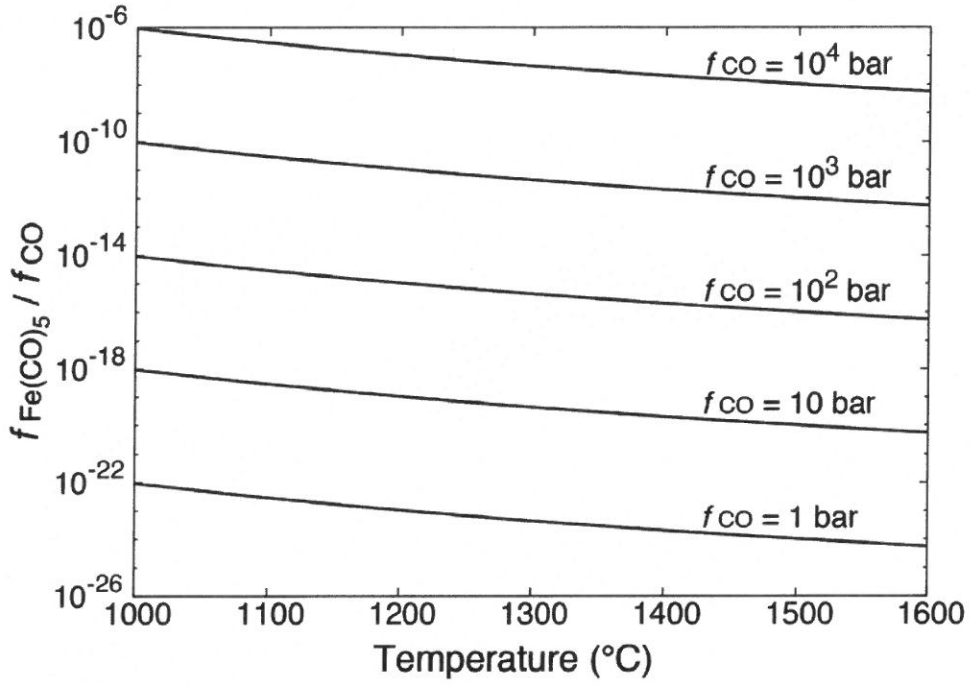

393
394

395 **Fig. 3.** Calculated ratio of the fugacity of $Fe(CO)_5$ to the fugacity of CO for various
396 temperatures and CO fugacities.